Multicarrier Code Division Multiplex with iterative MAP Symbol–by–Symbol Estimation

Frieder Sanzi, Alexander Slama, Joachim Speidel
Institute of Telecommunications, University of Stuttgart
Pfaffenwaldring 47, 70569 Stuttgart, Germany

***Abstract*— In this paper we consider a Multi Carrier Code Division Multiplex (MC–CDM) scheme. At the receiver side the Maximum A Posteriori Symbol–by–Symbol Estimator (MAPSSE) is used for the detection of the CDM signal. Therefore the influence of the spreading factor on the overall Bit Error Rate (BER) is investigated. We concatenate the MAPSSE with the channel decoder which allows for iterative decoding. This system can be considered as a serially concatenated iterative decoding scheme whereby the inner decoder is replaced by the MAPSSE. Therefore the bit error rate can be further reduced by means of iterative decoding. A combination with an inner Recursive Systematic Convolutional (RSC) component code with rate 1 is suggested to further improve performance. The applications are broadcasting and with some extensions two way communications.**

Keywords—**OFDM, CDMA, iterative decoding**

I. Introduction

For mobile communication systems Orthogonal Frequency Division Multiplexing (OFDM) has received a lot of attention in the recent years. Therefore OFDM has become an important modulation scheme for several applications, like Digital Subscriber Line (DSL), Digital Audio Broadcasting (DAB), Terrestrial Digital Video Broadcasting (DVB-T) and Wireless LAN (e.g. HYPERLAN). One advantage of OFDM is that it turns a frequency selective channel into a flat fading channel for each sub–carrier. So, the frequency domain equalizer is just a one tap equalizer for each sub–carrier. To achieve frequency diversity, OFDM can be combined with Code Division Multiplex (CDM), where the signal is spread over several sub–carriers. This concept was introduced as OFDM–CDMA or multicarrier CDMA (MC–CDMA) by [1], [2], [3] and is also called MC–spread spectrum (MC–SS).

In this paper the authors consider a MC-CDM system in which each receiver can decode the total bitrate by using all orthogonal codes. For the detection the maximum a posteriori symbol–by–symbol estimator (MAPSSE) is proposed. With this scheme we investigate the impact of the spreading factor on the overall bitrate. In recent time since the invention of Turbo Codes by [4] iterative decoding algorithms for spectrally efficient modulation have become a vital field of research in digital communication. In this paper we suggest an application of the Turbo Principle for iterative MAPSSE concatenated with the channel decoder. This system can be regarded as a serially concatenated iterative decoding scheme whereby the inner decoder is replaced by the MAPSSE. Often the reliability information of the channel decoder is used for soft–interference cancellation e.g. [5]. We propose to feed back this information directly to the MAPSSE stage. To further improve the performance of the system a combination with an inner RSC component code of rate 1 is suggested.

The performance of the proposed scheme is evaluated on the basis of bit error rate (BER) charts. In addition the convergence of the iterative decoding loop is studied with the Extrinsic Information Transfer Chart (EXIT Chart) recently introduced in [6], [7].

II. System Model

A. Transmitter

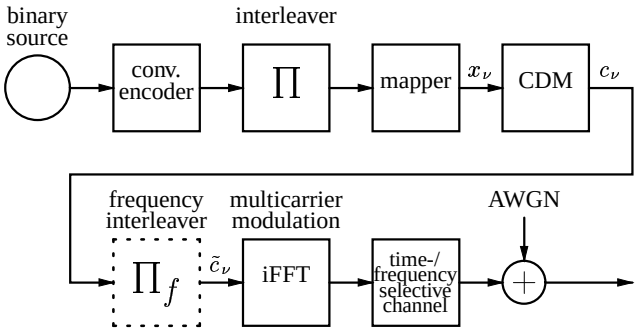

Fig. 1. Transmitter and channel model.

As shown in Fig. 1, the signal from the binary source is convolutionally encoded, interleaved, mapped (BPSK, alphabet ± 1) and spread by the CDM block, which takes N consecutive BPSK symbols x_ν, creates the vector $\tilde{\mathbf{B}}_{N\,m}$ with the coefficients $\tilde{b}_{\mu,m} = x_{N\cdot m+\mu}$ ($m \in \mathbf{Z}$ and $\mu = 0, 1, \ldots, N-1$) and multiplies it with the Walsh matrix $\mathbf{W}_N$.

$$\mathbf{B}^T_{N\,m} = \tilde{\mathbf{B}}^T_{N\,m} \cdot \mathbf{W}_N \tag{1}$$

The resulting vector $\mathbf{B}_{N\,m}$ with the coefficients $b_{\mu,m}$ is converted to the composite multicode CMD sequence c_ν with $c_\nu = b_{\nu \,\mathrm{MOD}\, N, \nu \,\mathrm{DIV}\, N}$ where DIV is integer division operator.

The set of N orthogonal Walsh–codes can be calculated recursively by using

$$\mathbf{W}_N = \frac{1}{\sqrt{N}} \begin{pmatrix} \mathbf{W}_{N/2} & \mathbf{W}_{N/2} \\ \mathbf{W}_{N/2} & -\mathbf{W}_{N/2} \end{pmatrix}, \qquad N \geq 2, \tag{2}$$

whereby $\mathbf{W}_1 = 1$ and $\mathbf{W}_N$ is the $N \times N$ Hadamard–Matrix [8] and N is the spreading factor.

The serial order of c_ν is interchanged by the subsequent interleaver which results in the sequence $\tilde{c}_\nu$. So the input $\tilde{c}_\nu$ to the multicarrier modulator is "frequency interleaved". $\tilde{c}_\nu$ is modulated onto K sub–carriers using iFFT.

For the following mathematical description, it is convenient to separate the discrete time axis into intervals of length K

$$\tilde{C}_{k,l} = \tilde{c}_{K\cdot l+k} \qquad , l \in \mathbf{Z}; k = 0, 1, \ldots, K-1 \tag{3}$$

and similarly for $C_{k,l}$ and $X_{k,l}$. The transmission is done on a block–by–block basis, with blocks of K sub–carriers in frequency and L OFDM symbols in time direction.

Global Telecommunications Conference, 2001. GLOBECOM '01. IEEE 25-29 November 2001, vol.2, pag 886 - 890

B. Channel Model

For the mobile channel we use the wide–sense stationary uncorrelated scattering (WSSUS) channel model introduced in [9]. The frequency response of the channel can be expressed as

$$H(f,t) = \frac{1}{\sqrt{M}} \sum_{i=1}^{M} e^{j(\varphi_i + 2\pi f_{D_i} t - 2\pi f \tau_i)}, \tag{4}$$

where φ_i is the phase, f_{D_i} the Doppler frequency and τ_i the delay of the ith path. The variable M denotes the number of propagation paths. The φ_i, f_{D_i} and τ_i are randomly chosen depending on the corresponding joint probability density function $p_{\varphi,f_D,\tau}(\varphi, f_D, \tau)$ of the considered channel model. We assume a channel model where the phase φ_i is uniformly distributed, the delay τ_i is exponentially distributed with probability density function (PDF) $p(\tau)$ and the Doppler shift f_{D_i} is distributed according to Jakes' power spectral density function. In this case the auto–correlation function in time is

$$R_{t;l} = J_0(2\pi f_{D_{max}} \cdot l \cdot T_s) \tag{5}$$

whereby $J_0()$ is the Bessel function, T_s is the duration of one OFDM symbol (useful part plus guard interval), l is the discrete time index and $f_{D_{max}}$ is the maximal Doppler shift. The complex auto–correlation function in frequency direction writes as

$$R_{f;k} = \frac{1 - e^{-\tau_{max}(\frac{1}{\tau_{rms}} + j2\pi \cdot k \cdot \Delta f)}}{(1 - e^{-\frac{\tau_{max}}{\tau_{rms}}}) \cdot (1 + j2\pi \cdot k \cdot \Delta f \cdot \tau_{rms})} \tag{6}$$

whereby τ_{max} is the channel delay spread, Δf is the sub–carrier spacing and k is the discrete frequency index. τ_{rms} is chosen such that $p(\tau_{max})/p(0) = 1/1000$.

C. Receiver

After multicarrier demodulation of the K sub–carriers and frequency deinterleaving, the received signal is fed into the MAPSSE stage (Fig. 2).

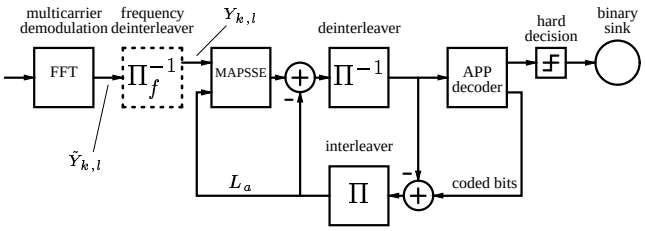

Fig. 2. Receiver, iterative MAPSSE and decoding.

The MAPSSE stage outputs a log–likelihood ratio value (L–value, see [10]) for each coded bit. After deinterleaving and soft–in/soft–out decoding with an A Posteriori Probability calculator (APP or MAP calculator, see [11]) the estimates on the transmitted bits are available at the output of the hard decision device. This can be accomplished by just considering the sign of the APP decoder soft output values. To allow for turbo processing with iterative MAPSSE and decoding, the extrinsic information on the coded bits is fed back from the APP decoder, and after interleaving it becomes *a priori* knowledge L_a for the MAPSSE stage.

III. MAPSSE WITH A PRIORI KNOWLEDGE

For our further considerations we assume the channel characteristic to be approximately unchanged during the duration of one OFDM symbol. Under this assumption and provided that the guard interval is longer than the delay spread of the channel the cyclic prefix avoids inter–carrier interference (ICI) and also inter–symbol interference (ISI). In this case we can compute the received composite multicode chip after multicarrier demodulation as

$$\tilde{Y}_{k,l} = \tilde{H}_{k,l} \cdot \tilde{C}_{k,l} + N_{k,l} \tag{7}$$

whereby l is the OFDM symbol index, k is the sub–carrier index, $\tilde{C}_{k,l}$ are the transmitted composite multicode chips and $N_{k,l}$ are independent and identically distributed complex Gaussian noise variables with component–wise noise power $\sigma_n^2 = N_0/2$. The $\tilde{H}_{k,l}$ are sample values of the channel frequency response.

$$\tilde{H}_{k,l} = H(k\,\Delta f, l\,T_s) \tag{8}$$

After the frequency deinterleaver the signal writes as

$$Y_{k,l} = H_{k,l} \cdot C_{k,l} + N_{F_{\Pi_f}^{-1}(k),l}, \tag{9}$$

whereby $H_{k,l} = \tilde{H}_{F_{\Pi_f}^{-1}(k),l}$ and $F_{\Pi_f}^{-1}$ denotes the inverse operation of the frequency interleaver. Note that this interleaver operates only in frequency direction (permutes the composite multicode chips on the sub–carriers) and not in time direction.

The MAPSSE operates blockwise and takes N received composite multicode chips $Y_{k,l}$ which are grouped in a vector $\mathbf{Y}$ and outputs N L–values on the BPSK symbols $X_{k,l}$ which are also called coded bits in the following. For simplification we just write X_μ for the coded bits, H_μ for the channel state information, C_μ for the composite multicode chips ($\mu \in \{0, \cdots, N-1\}$) and $\mathbf{Y}^T = \{Y_0, \cdots, Y_{N-1}\}$.

First, we consider a simple example with $N = 2$ to get an idea of the principles on the MAPSSE–algorithm. In this case the MAPSSE block needs to calculate L–values on the coded bits X_0, X_1 for each incoming vector $\mathbf{Y}$. The L-value of bit X_0 conditioned on $\mathbf{Y}$ can be calculated as follows (see [12]).

$$L(X_0|\mathbf{Y}) = \begin{array}{l} L_a(X_0) \\ + \ln \frac{p(\mathbf{Y}|X_0=1,X_1=-1) + p(\mathbf{Y}|X_0=1,X_1=1) \cdot \exp L_a(X_1)}{p(\mathbf{Y}|X_0=-1,X_1=-1) + p(\mathbf{Y}|X_0=-1,X_1=1) \cdot \exp L_a(X_1)} \end{array} \tag{10}$$

The *a priori* L-values write as

$$L_a(X_0) = \ln \frac{\Pr(X_0 = 1)}{\Pr(X_0 = -1)}, L_a(X_1) \quad \text{respectively.} \tag{11}$$

The conditional probability density function in (10) is given by (see [13])

$$p(\mathbf{Y}|X_0,X_1) = \frac{1}{(2\pi\sigma_n^2)^2} \exp[-\frac{1}{2\sigma_n^2}(|Y_0 - H_0 \cdot C_0|^2 + |Y_1 - H_1 \cdot C_1|^2)] \tag{12}$$

whereby

$$(C_0, C_1) = (X_0, X_1) \cdot \mathbf{W}_2. \tag{13}$$

Putting (12) into (10) we obtain the L–value on the coded bit X_0 and X_1, respectively.

For a given spreading factor N we obtain the L–value of the coded bit X_μ as follows (see [12])

$$L(X_\mu|\mathbf{Y}) - L_a(X_\mu) = \ln \frac{\sum_{i=0}^{2^{N-1}-1} p\left(\mathbf{Y}|X_\mu=1, X_{j,j=0,\ldots,N-1,j\neq\mu} \equiv \mathrm{abin}(i)\right) \cdot \exp \sum_{\substack{j=0,j\neq\mu \\ \mathrm{b}(i,h)=1}}^{N-1} L_a(X_j)}{\sum_{i=0}^{2^{N-1}-1} p\left(\mathbf{Y}|X_\mu=-1, X_{j,j=0,\ldots,N-1,j\neq\mu} \equiv \mathrm{abin}(i)\right) \cdot \exp \sum_{\substack{j=0,j\neq\mu \\ \mathrm{b}(i,h)=1}}^{N-1} L_a(X_j)} \tag{14}$$

whereby $X_{j,j=0,\ldots,N-1,j\neq\mu} \equiv \mathrm{abin}(i)$ denotes the joint event of the variables $X_{j,j=0,\ldots,N-1,j\neq\mu}$ having the values $-1, 1$ according to $\mathrm{abin}(i)$ with $\mathrm{abin}(i) = 2 \cdot \mathrm{bin}(i) - 1$ and $\mathrm{bin}(i)$ being the binary decomposition of i. The function $b(i,h)$ takes on the value $'1'$ if bit number h is set in the binary decomposition of i, otherwise it is $'0'$, with

$$h = \begin{cases} j & ;j < \mu \\ j-1 & ;j \geq \mu \end{cases} . \tag{15}$$

According to (12) the conditional probability density function writes as

$$p(\mathbf{Y}|X_0,\ldots,X_{N-1}) = \frac{1}{(2\pi\sigma_n^2)^N} \exp\left[-\frac{1}{2\sigma_n^2} \sum_{i=0}^{N-1} |Y_i - H_i \cdot C_i|^2\right] \tag{16}$$

whereby

$$(C_0,\ldots,C_{N-1}) = (X_0,\ldots,X_{N-1}) \cdot \mathbf{W}_N. \tag{17}$$

IV. Inserting an inner RSC component code

We can further improve the performance of the iterative decoding loop by inserting an inner RSC component code of rate 1 at the transmitter. Fig. 3 shows the necessary changes at the transmitter.

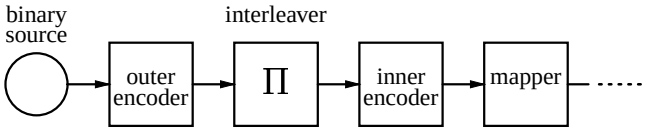

Fig. 3. Modified transmitter with inner RSC code.

We introduce a special puncturing scheme to make use of RSC component codes with small memory and low decoding complexity. Fig. 4 illustrates the concept of "heavy puncturing": Most of the parity bits (sometimes also referred to as coded bits) of the rate $1/2$ RSC mother code are discarded, such that from the total of n_s parity bits only n_p remain. The parity bits are periodically inserted into the systematic bit stream in such a way, that they replace the information bits at these positions. Therefore we obtain a rate 1 code with $n_s - n_p$ information bits and n_p parity bits. The insertion period ΔP of the parity bits is $\Delta P = n_s/n_p$.

Owing to the heavy puncturing $n_p < n_s$ (code structure almost destroyed) the error correcting capabilities of the inner decoder are very poor. However, we noticed that particularly those properties which are crucial for good iterative decoding performance, are still preserved, as will be further detailed in Section V-B.

In Fig. 5 the necessary changes at the receiver are shown.

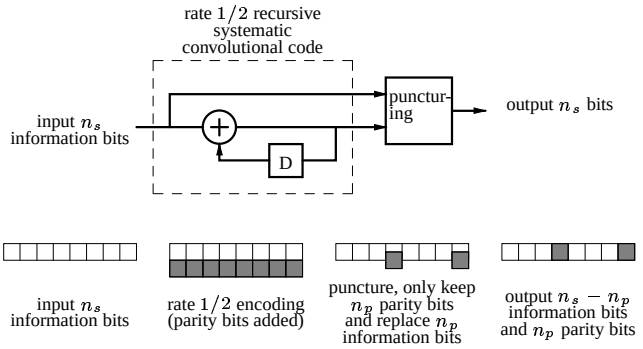

Fig. 4. Puncturing scheme of inner rate $1/2$ mother code; $n_s = 8$, $n_p = 2$.

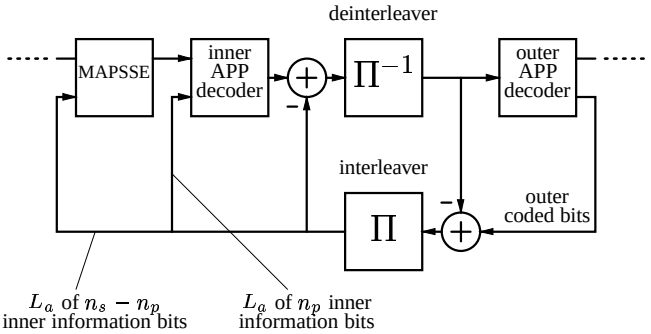

Fig. 5. Modified receiver with inner APP decoder.

The extrinsic information on the coded bits is fed back from the outer APP decoder, and after interleaving it becomes *a priori* knowledge L_a on the inner information bits (n_s bits). The *a priori* knowledge L_a for the MAPSSE stage should be on $n_s - n_p$ inner information bits and on n_p inner parity bits. Because there is no *a priori* knowledge on the inner parity bits, we can only use the *a priori* knowledge on the $n_s - n_p$ inner information bits for the MAPSSE stage. The output of the MAPSSE stage becomes the input of the inner APP decoder with $n_s - n_p$ L–values on the inner information bits and n_p L–values on the parity bits. Additionally, we can use the remaining *a priori* knowledge on the n_p inner information bits for the inner APP decoder which is not fed to the MAPSSE stage. Therefore the whole *a priori* knowledge is used which is fed back from the outer APP decoder.

V. Simulation Results

We use the following channel and multicarrier system parameters: duration of one OFDM–symbol $T_s = 300\mu$s, sub–carrier spacing $\Delta f = 4$kHz, channel delay spread $\tau_{max} = 20\mu$s and maximal Doppler shift $f_{D_{max}} = 100$Hz. With $K = 1024$ adjacent sub–carriers, $L = 100$ consecutive OFDM symbols in time, the interleaving depth is $L \cdot K = 102400$ (outer) coded bits and the frequency interleaving depth is $K = 1024$.

BER charts are used for performance analysis of different system configurations. In addition to that, we apply the Extrinsic Information Transfer Chart (EXIT chart) to better compare the different system configurations and to gain more insight into the convergence behavior of iterative decoding.

The (outer) convolutional code is recursive systematic with feedback polynomial $G_r = 037$, feedforward polynomial $G = 023$ and code rate $R_c = 0.5$. We further assume, that

the channel state information $H_{k,l}$ is perfectly known at the receiver side. Channel estimation for a MC–CDMA system can be accomplished by inserting pilot symbols into the transmitted data stream (see [14]).

A. Without inner code

Fig. 6 shows mutual information transfer characteristics of the MAPSSE stage. The *a priori* input to the MAPSSE is on the abscissa (mutual information $0 \leq I_{A_1} \leq 1$ in bit per binary symbol). The *a posteriori* output is on the ordinate (mutual information $0 \leq I_{E_1} \leq 1$). Mutual information transfer characteristics describe the input/output relations of the MAPSSE and are calculated by applying a Gaussian distributed random variable as *a priori* input and quantifying the *a posteriori* output in terms of mutual information [6], [7].

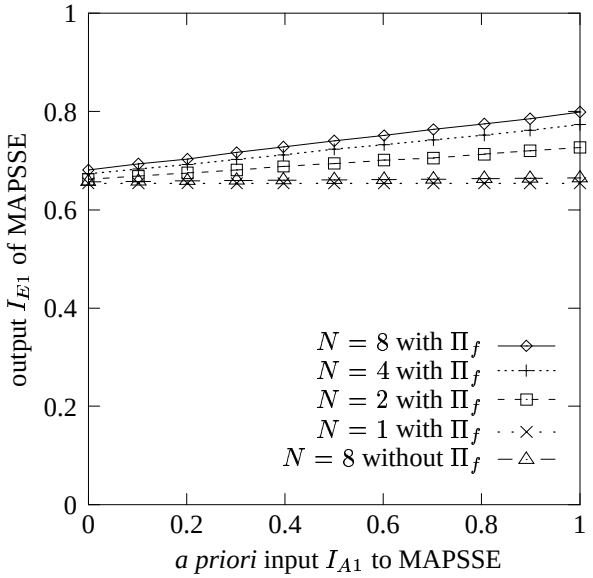

Fig. 6. Mutual information transfer characteristics of MAPSSE stage for different spreading factor and with or without frequency interleaver Π_f ($E_b/N_0 = 4.5\text{dB}$).

As can be seen the curves are straight lines. Increasing the spreading factor N results in a higher ascending slope and also the curves start for no *a priori* knowledge I_{A1} (very left side of chart) at a higher *a posteriori* output I_{E1} for a system with frequency interleaver Π_f . For $N = 1$ the ascending slope of the curve is zero. Therefore this system can not be improved by means of iterative decoding. A similar result is achieved if there is no frequency interleaver Π_f. As can be seen from Fig. 6 for the case $N = 8$ the ascending slope is nearly zero. We can summarize the results as follows: A frequency interleaver Π_f demolishes the orthogonality of the Walsh–Codes, but this results in a better diversity gain and the system can be improved by means of iterative decoding. Whereas in a system without frequency interleaver Π_f the orthogonality nearly remains, but there is almost no possibility of system improvement by means of iterative decoding. In addition the diversity gain is smaller.

The trajectory of iterative decoding shows the exchange of channel and extrinsic information between MAPSSE stage and decoder. In Fig. 7 the EXIT Chart is depicted. The trajectory is a simulation result of the iterative scheme, whereas the transfer characteristics are computed individually for the inner MAPSSE stage and the outer decoder, applying independent Gaussian distributed random variables as *a priori* inputs. The achieved trajectory matches with the characteristics fairly well. After about 3 iterations the trajectory gets stuck, owing to the intersection of both characteristics.

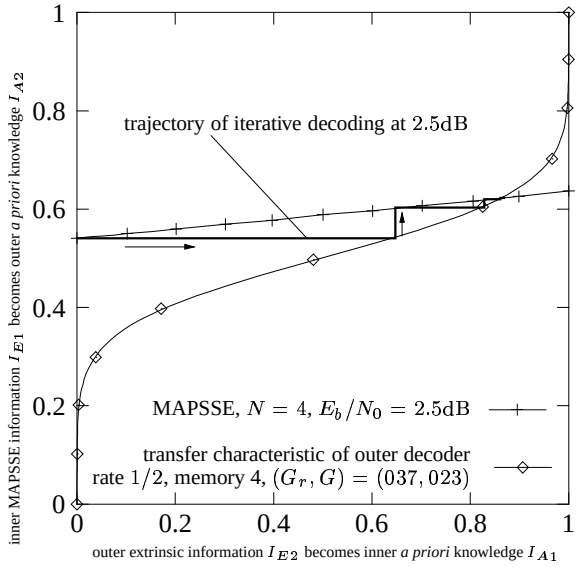

Fig. 7. EXIT chart, MAPSSE ($N = 4$, with Π_f) and outer memory 4 decoder with simulated trajectory of iterative decoding at $E_b/N_0 = 2.5\text{dB}$.

The BER chart of Fig. 8 shows the system performance for spreading factor $N = 8$, with or without frequency interleaver Π_f and for different numbers of iterations.

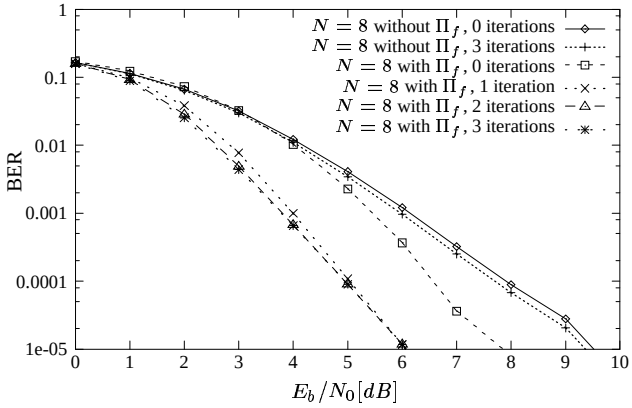

Fig. 8. BER curves of system with or without frequency interleaver Π_f for $N = 8$.

As can be seen for the system without frequency interleaver Π_f the improvement of the iterative decoding loop is low, whereas for the system with frequency interleaver Π_f a remarkable improvement is achieved. At BER 10^{-4} the gain between the curve for 2 iterations and the curve for 0 iterations is about 1.8dB. We can also conclude that for the system with frequency interleaver Π_f almost 2 iterations are enough.

In Fig. 9 the system performance with frequency interleaver is shown after 2 iterations for different spreading factors N except for $N = 1$. In the case $N = 1$ no improvement is achieved

with the iterative decoding loop.

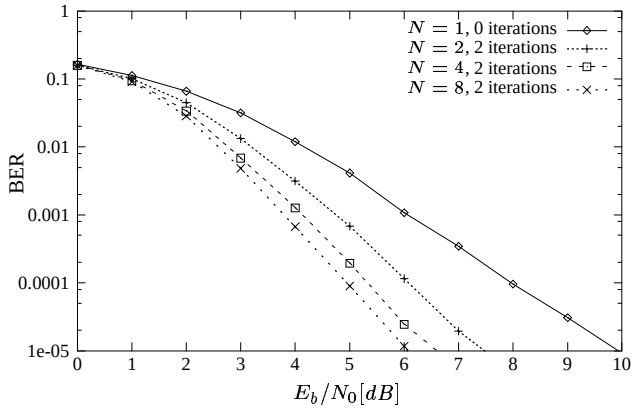

Fig. 9. BER curves of system with frequency interleaver Π_f for different spreading factors.

The BER chart of Fig. 9 illustrates the performance improvement by increasing the spreading factor N. The gain between spreading factor $N = 8$ and $N = 1$ (no spreading) is about 3dB at BER 10^{-4}. But we have to note that the complexity of the MAPSSE stage increases exponentially for increasing the spreading factor N.

B. With inner code

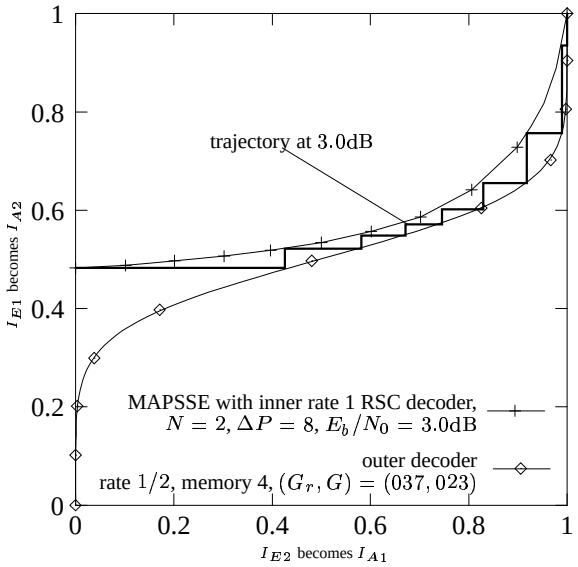

Fig. 10. EXIT chart of MAPSSE ($N = 2$) and inner rate one RSC decoder ($\Delta P = 8$) in combination with outer memory 4 decoder; decoding trajectory at $E_b/N_0 = 3.0$dB.

The iterative MAPSSE and decoding loop of the system with inner decoder can be studied in the EXIT chart of Fig. 10 for one particular block ($K = 1024$, $L = 100$). We choose $\Delta P = 8$ for "heavy puncturing". The decoding trajectory at $E_b/N_0 = 3.0$dB, spreading factor $N = 2$, can converge towards $(I_{A1}, I_{E1}) \approx (1, 1)$, which directly relates to reaching a very low BER.

The BER curves of Fig. 11 show a steep "turbo cliff". At a BER of 10^{-4} the advantage to the system without inner code is about 3.0dB for $N = 4$ and also 3.0dB for $N = 2$.

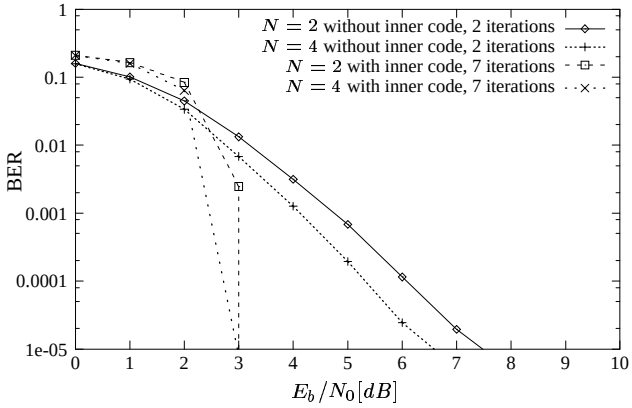

Fig. 11. BER chart of the system with inner decoder; for better comparison, two reference curves are copied from Fig. 9.

VI. Conclusion

We have shown that the use of the MAPSSE concatenated with an outer channel decoder can reduce the BER by means of iterative decoding. A performance gain of about 3.0dB is achieved by increasing the CDM spreading factor N from 1 to 8. The system performance of the iterative decoding loop can be further improved by about 3.0dB with an additional inner rate one RSC component code.

References

[1] N. Yee, J.–P. Linnartz and G. Fettweis, "Multi–Carrier CDMA in Indoor Wireless Radio Networks", *Proc. IEEE Int. Symp. on Personal, Indoor and Mobile Radio Commun. (PIMRC)*, pp. D1.3.1–D1.3.5, September 1993

[2] G. Fettweis, A. Shaikh Babai and K. Anvari, "On Multi–Carrier Code Division Multiple Access (MC–CDMA) Modem Design", *Proc. IEEE Vehicular Technology Conference (VTC)*, pp. 1670–1674, June 1994

[3] K. Fazel, "Performance of CDMA/OFDM for Mobile Communication System", *Proc. IEEE Int. Conf. on Universal Personal Commun. (ICUPC)*, pp. 975–979, October 1993

[4] C. Berrou, A. Glavieux and P. Thitimajshima, "Near Shannon limit error–correcting coding and decoding: Turbo–codes", *Proc. IEEE Int. Conf. on Commun. (ICC), Geneva, Switzerland*, pp. 1064–1070, May 1993

[5] S. Kaiser and J. Hagenauer, "Multi–carrier CDMA with Iterative Decoding and Soft–Interference Cancellation", *Proc. IEEE Global Telecommun. Conf. (Globecom), Phoenix, USA*, pp. 6–10, November 1997

[6] S. ten Brink, "Iterative Decoding Trajectories of Parallel Concatenated Codes", *Proc. 3rd IEEE/ITG Conf. on Source and Channel Coding, Munich, Germany*, pp. 75–80, January 2000

[7] S. ten Brink, "Design of Serially Concatenated Codes based on Iterative Decoding Convergence", *2nd International Symposium on Turbo Codes, Brest, France*, pp. 319–322, September 2000

[8] J. G. Proakis, "Digital Communication", *McGraw–Hill, 3rd edition*, 1995

[9] P. Hoeher, "A Statistical Discrete-time model for the WSSUS multipath channel", *IEEE Trans. on Veh. Tech.*, vol 41, pp. 461–468, Nov. 1992

[10] J. Hagenauer, E. Offer, L. Papke, "Iterative Decoding of Binary Block and Convolutional Codes", *IEEE Trans. Inform. Theory*, vol. 42, no. 2, pp. 429–445, March 1996

[11] L. Bahl, J. Cocke, F. Jelinek, J. Raviv, "Optimal decoding of linear codes for minimizing symbol error rate", *IEEE Trans. Inform. Theory*, vol. 20, pp. 284–287, Mar. 1974

[12] S. ten Brink, J. Speidel, R.-H. Yan "Iterative Demapping and Decoding for Multilevel Modulation", *Proc. IEEE Global Telecommun. Conf. (Globecom), Sydney, Australia*, pp. 579–584, November 1998

[13] S. ten Brink, J. Speidel, R.-H. Yan, "Iterative demapping for QPSK modulation", *IEE Electronic Letters*, vol. 34, no. 15, pp. 1459–1460, July 1998

[14] P. Hoeher, S. Kaiser, P. Robertson, "Two–dimensional pilot–symbol–aided channel estimation by Wiener filtering", *Proc. ICASSP*, pp. 1845–1848, April 1997